

MicroRNA-1224 inhibits cell proliferation by downregulating CBX3 expression in chordoma

WEI XIA, JIHE HUANG, CHUNHUA SUN, FEI SHEN and KEJIA YANG

Department of Orthopedics, Suzhou Wuzhong People's Hospital, Suzhou, Jiangsu 215128, P.R. China

Received August 15, 2023; Accepted March 15, 2024

DOI: 10.3892/ol.2024.14395

Abstract. MicroRNAs (miRNAs/miRs) have abnormal expression in numerous tumors and are closely related to tumor development and resistance to radiotherapy and chemotherapy. However, there are few studies assessing the role and mechanism of miRNA in chordoma. The sequencing data of three pairs of chordoma and notochord tissues from the GSE56183 dataset were analyzed in the present study. Cell proliferation was assessed *in vitro* using Cell Counting Kit-8. Bioinformatics analysis and the dual luciferase reporter assay were used to evaluate the regulatory relationship between miR-1224 and chromobox 3 (CBX3) in chordoma. The results demonstrated that miR-1224 had a significantly lower expression level in chordoma tissues and cell lines. Overexpression of miR-1224 inhibited proliferation in the chordoma cells, while the knockdown of miR-1224 promoted proliferation of the chordoma cells. Bioinformatics analysis and the dual luciferase reporter assay confirmed that CBX3 was a direct target gene of miR-1224 and that miR-1224 induced the proliferation of chordoma cells through the inhibition of CBX3. In summary, miR-1224 reduced the proliferation of chordoma cells through inhibition of CBX3, which provides a theoretical basis for selecting a novel therapeutic target for chordoma.

Introduction

Chordoma is a relatively common primary malignant bone tumor of the spine; it is mainly derived from notochord tissues that are not completely degenerated and frequently occurs in elderly individuals (1). In the last decade, the incidence rate of chordoma was approximately one to two cases per million individuals each year across all countries, with a slightly higher frequency in males than in females (2). Due to the special and complex anatomical structure of the spinal cord, radical tumor resection is difficult in most cases, and

chordoma is not sensitive to radiotherapy or chemotherapy. Therefore, the local recurrence rate of chordoma is as high as 50-70% after surgery (3). Chordoma remains a major clinical problem in the field of tumor surgery, which is extremely challenging. Further research is required to further explore the pathogenesis of chordoma to produce more effective interventions and treatment methods to improve the clinical efficacy. With the successful application of molecular targeted therapy in tumors, practical ideas have been offered for the targeted therapy of chordoma (4).

With the decrease in the cost of whole-genome sequencing techniques, more studies have confirmed that non-coding RNAs, especially microRNAs (miRNAs/miRs) (5-7), serve roles in the treatment of tumors. miRNAs are a group of endogenous short non-coding RNAs that are 21-25 nucleotides in length, which regulate the expression of target genes by specifically degrading or inhibiting the translation of target mRNA, thereby regulating cell growth, proliferation, apoptosis, metastasis, cycle distribution and differentiation (5,8). miRNAs have abnormal expression in numerous tumors, and are closely related to tumor development and resistance to radiotherapy and chemotherapy (9-13). However, miRNAs are rarely studied in chordoma. In the present study, the differential expression of miRNAs in three pairs of chordoma and notochord tissues from the GSE56183 dataset were studied.

The functional roles of differential expression of miRNAs in regulating the proliferation of chordoma cell lines were assessed in the present study, and the underlying molecular mechanisms were explored.

Materials and methods

Microarray data. The expression levels of miRNAs in chordoma and notochord tissues were downloaded from the GEO database (accession no. GSE56183; <http://www.ncbi.nlm.nih.gov/geo/>). The GSE56183 dataset contains three pairs of chordoma and notochord tissues (14). The data were processed using R (version 3.2.5; R Core Team). The cut-off level was fold change ≥ 1.5 and $P < 0.05$ was used to indicate significant differences.

Cell transfection. Human chordoma JHC7 (CRL-3267), U-CH1 (CRL-3217) and U-CH2 (CRL-3218) cell lines and immortalized nucleus pulposus NP1 (BFN60808675) and NP2 (BFN608007213) cell lines were purchased from the

Correspondence to: Dr Kejia Yang, Department of Orthopedics, Suzhou Wuzhong People's Hospital, 61 Dongwu North Road, Wuzhong, Suzhou, Jiangsu 215128, P.R. China
E-mail: yangkejia198676@163.com

Key words: miR-1224, CBX3, chordoma

American Type Culture Collection by BFB Life Sciences [Qingqi (Shanghai) Biotechnology Development Co., Ltd.]. The pMSCV-puro plasmid negative control (NC), chromobox 3 (CBX3) overexpression plasmid, CBX3 small interfering (si)RNA, non-targeting double-stranded NC siRNA, miRNA NC mimics, miR-1224 mimics, miRNA NC inhibitors and miR-1224 inhibitors were purchased from Guangzhou RiboBio Co., Ltd. The cells were cultured at 37°C with 5% CO₂ and transfected with Lipofectamine 2000® (Thermo Fisher Scientific, Inc.) for 6 h at 37°C with 5% CO₂, and the medium was then replaced with fresh culture medium, according to the manufacturer's instructions. The transfection efficiency was observed under a fluorescence microscope at 24 h after transfection and was used to determine whether subsequent experiments were to be performed. The sense and antisense sequences of siRNA CBX3 were designed with online siRNA design tool siRNA selection Program (https://sirna.wi.mit.edu/sirna_search.cgi) using the coding sequences of CBX3 transcript (NM_016587.4).

The miRNA NC mimic (cat. no. HY-R04602), miR-1224 mimic (cat. no. HY-R00114), miRNA NC inhibitor (cat. no. HY-RI04602) and miR-1224 inhibitor (cat. no. HY-RI00114) were originally designed by MedChemExpress (purchased by Guangzhou RiboBio Co., Ltd.). The sense and antisense sequences of siRNA CBX3, miR-1224 mimics and miR-1224 inhibitors, including the NCs, are shown in Table SI.

Reverse transcription-quantitative (RT-q)PCR. Total RNA was extracted from JHC7, U-CH1 and U-CH2 cell lines, and from nucleus pulposus NP1 and NP2 cells using TRIzol® (Thermo Fisher Scientific, Inc.) and reverse transcribed into cDNA using the Transcriptor First Strand cDNA Synthesis Kit (Roche Applied Science) according to the manufacturer's instructions. RT-qPCR was performed using the SYBR Green Realmaster Mix Kit (Tiangen Biotech Co., Ltd.) and ABI ViiA 7 PCR system (Applied Biosystems; Thermo Fisher Scientific, Inc.). The following thermocycling conditions were used for qPCR: Initial denaturation at 95°C for 10 min, followed by 40 cycles of 95°C for 15 sec, 60°C for 30 sec and 2°C for 30 sec. Finally, melting curve analysis was performed with temperature ramping from 65 to 95°C at a rate of 0.5°C/sec with continuous fluorescence acquisition. The expression levels of miRNAs and mRNAs were quantified using the 2^{-ΔΔC_q} method (15) and normalized to the internal reference genes GAPDH and U6 for mRNA and miRNA, respectively. The primer design for miR-1224 was based on a study by Hu *et al* (16). All primers are shown in Table SII.

Western blotting. At 48 h after transfection, total protein was extracted from NP1, NP2, JHC7 and U-CH1 cells with RIPA reagent (Beyotime Institute of Biotechnology) and the protein concentration was determined by BCA kit (Beyotime Institute of Biotechnology). Next, 30 μg of the protein was loaded per lane and separated on 12% gels using SDS-PAGE. The separated proteins were transferred onto a PVDF membrane at 110 V for 2 h. The membrane was blocked with 5% skimmed milk powder in TBST for 1 h at 25°C and incubated with anti-CBX3 (1:2,000; cat. no. ab217999; Abcam) and anti-GAPDH (1:5,000; cat. no. ab201822; Abcam) primary antibodies at 4°C overnight

on a shaker. After the membrane was washed with TBST (0.1% Tween-20) three times (10 min/wash), the membrane was incubated with the secondary anti-rabbit IgG HRP-linked antibody (1:3,000; cat. no. 7076; Cell Signaling Technology, Inc.) at room temperature for 1 h on a shaker. After the membrane was washed with TBST three times (10 min/wash), the protein bands were developed with ECL developing solution (Abcam). The expression of the target protein was analyzed with ImageJ software (version 1.54i; National Institutes of Health) and normalized to GAPDH.

Dual luciferase reporter assay. The target genes of miR-1224 were predicted using TargetScan (http://www.targetscan.org/vert_72/), microRNAorg (<http://www.microrna.org/microrna/home.do>) and RegRNA2.0 (<http://regrna2.mbc.nctu.edu.tw/detection.html>) databases. The wild-type (WT) and mutant (MUT) fluorescence plasmids, psiCheck2-CBX3 3'-untranslated region (3'UTR)-WT and psiCheck2-CBX3 3'UTR-MUT (Generbiol), were constructed. The miRNA NC mimic, miR-1224 mimic and psiCheck2-CBX3 3'UTR-WT or psiCheck2-CBX3 3'UTR-MUT vector were transfected into the JHC7 cells along with a *Renilla* luciferase control vector using Lipofectamine 3000 (Thermo Fisher Scientific, Inc.) according to the manufacturer's protocol. The transfected cells were incubated for 24 h to allow for protein expression and promoter activity. The luciferase activity was measured using the Dual-Luciferase Reporter Assay System (Promega Corporation). The ratio of firefly luciferase activity to *Renilla* luciferase activity was calculated to normalize for transfection efficiency and variations in cell number. The firefly luciferase activity was normalized to the internal control (*Renilla* luciferase) activity for each sample. The normalized firefly luciferase activity was expressed as relative luciferase units or fold-change compared with control samples.

Cell Count Kit-8 (CCK-8) cell proliferation activity assay. Cell proliferation was measured using a CCK-8 kit (Dojindo Laboratories, Inc.). The cells were seeded at 1x10⁴ cells/well into a 96-well plate and incubated for 24 h with 5% CO₂ at 37°C. Next, 20 μl CCK-8 solution was added and the cells were incubated at 37°C for 4 h. The absorbance value of the two groups at 490 nm was measured using a microplate reader at 0, 24, 48 and 72 h. The experiment was repeated three times.

Statistical methods. SPSS 22.0 (IBM Corp.) and GraphPad Prism 6.0 software (Dotmatics) were used for data analysis. Data are expressed as the mean ± standard deviation. The differences between two groups were tested using an unpaired Student's t-test, and one-way analysis of variance with Tukey's Honestly Significant Difference post hoc test was used for the analysis of >2 groups. P<0.05 was considered to indicate a statistically significant difference.

Results

Differential expression of miRNA in chordoma. To assess the differential expression of miRNAs in chordoma, the sequencing data of three pairs of chordoma and notochord tissues from the GSE56183 dataset were analyzed. A total of 1,109 human miRNAs were detected in GSE56183. Using cut

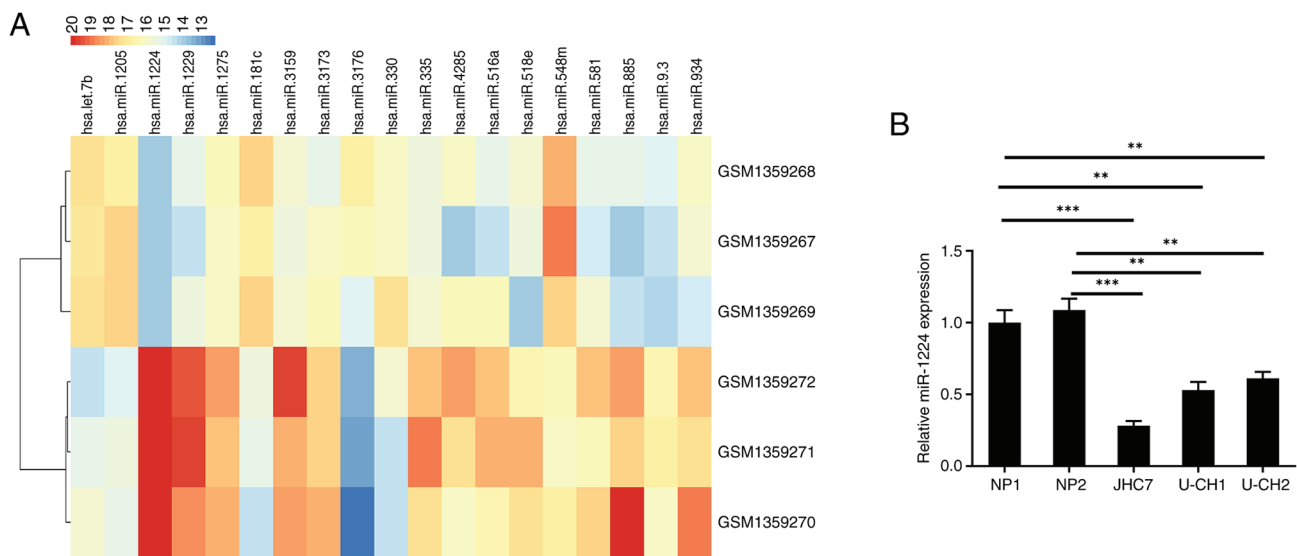


Figure 1. (A) Analysis of differentially expressed miRNAs based on three pairs of chordoma (GSM1359268, GSM1359267 and GSM1359269) and notochord tissues (GSM1359272, GSM1359271 and GSM1359270) from the GSE56183 dataset. Fold-change ≥ 1.5 and $P < 0.05$ were cutoff values for differential expression. Data are expressed as fragments per kilobase of exon model per million mapped fragments. (B) Expression of miR-1224 in chordoma JHC7, U-CH1 and U-CH2 cell lines, and nucleus pulposus NP1 and NP2 cell lines. ** $P < 0.01$ and *** $P < 0.001$. miR, microRNA.

off values of fold-change (FC) ≥ 1.5 and $P < 0.05$, 19 miRNAs were demonstrated to be differentially expressed in chordoma. miR-1224, miR-1229, miR-885, miR-3159, miR-934, miR-335, miR-518e, miR-516a, miR-9.3, miR-581, miR-4285, miR-3173 and miR-1275 were expressed at low levels in chordoma compared with notochord tissues, while miR-3176, miR-181c, miR-1205, let-7b, miR-330 and miR-548m were highly expressed in chordoma (Fig. 1A). The differential expression of miR-1224 in chordoma was the most apparent. From this, the expression of miR-1224 in chordoma JHC7, U-CH1 and U-CH2 cell lines, and normal NP1 and NP2 cell lines, was detected. These results demonstrated that miR-1224 also had significantly lower expression in chordoma cells compared with nucleus pulposus cells (Fig. 1B).

Effects of miR-1224 on the proliferation ability of chordoma cells. miR-1224 expression was lower in JHC7 and U-CH1 cells compared with U-CH2 cells. Therefore, JHC7 and U-CH1 were selected for subsequent experiments (Fig. 1B). The chordoma JHC7 and U-CH1 cell lines were transfected with the miR-1224 mimic and miRNA NC mimic, and the expression of miR-1224 in these cells was detected using RT-qPCR. The RT-qPCR results demonstrated that the expression levels of miR-1224 in the miR-1224 mimic groups in both cell lines were significantly higher compared with those in the respective miR-NC group (Fig. 2A). Likewise, the CCK-8 proliferation assay demonstrated that the proliferation levels of the JHC7 (Fig. 2B) and U-CH1 (Fig. 2C) cells with miR-1224 mimic were significantly lower compared with the levels of the respective controls. Furthermore, the miR-1224 inhibitor and miR-1224 inhibitor NC were transfected into the JHC7 and U-CH1 chordoma cell lines. At 48 h after transfection, the expression of miR-1224 was detected using RT-qPCR. The expression levels of miR-1224 in the miR-1224 inhibitor groups were significantly lower compared with those in the respective controls (Fig. 2D). Likewise, the CCK-8 proliferation assay

demonstrated that after miR-1224 expression was down-regulated, the cell proliferation levels of JHC7 (Fig. 2E) and U-CH1 (Fig. 2F) were significantly higher compared with those of the respective controls. Overall, this suggested that miR-1224 could inhibit the proliferation of chordoma and serve as a tumor suppressor.

Screening and validation of miR-1224 target genes. The target genes of miR-1224 were predicted using TargetScan, microRNAorg and RegRNA2.0 databases, and TMEM221, TUBB2A, LBP, CBX3 and MED20 were selected. The chordoma JHC7 and U-CH1 cells were transfected with the miR-1224 mimic and miR-1224 mimic NC, and RT-qPCR was used to detect the mRNA expression of candidate target genes. From these target genes, only the mRNA expression of CBX3 was significantly decreased compared with the control (Fig. 3A and B).

Furthermore, western blotting demonstrated that the protein expression of CBX3 also decreased in both cell lines transfected with the mimic compared with the miRNA NC mimic (Fig. 3C). Moreover, the miR-1224 inhibitor and miR-1224 inhibitor NC were transfected into JHC7 (Fig. 3D) and U-CH1 (Fig. 3E) chordoma cell lines, and RT-qPCR demonstrated that from the target genes, only the mRNA expression of CBX3 was significantly increased compared with that of the control. Likewise, western blotting demonstrated that the protein expression of CBX3 also decreased in both cell lines compared with the miRNA NC inhibitor (Fig. 3F).

Based on the aforementioned results, it was suggested that CBX3 could be a target of miR-1224. To further confirm whether CBX3 is a direct target of miR-1224, CBX3 3'UTR-WT and 3'UTR-MUT luciferase expression vectors were constructed (Fig. 3G). Luciferase expression vectors with WT or MUT 3'-UTRs were co-transfected with either the miR-1224 mimic or the miR-1224 mimic NC in JHC7 cells. The results of the dual luciferase reporter assay demonstrated that co-transfection of miR-1224 with WT 3'-UTR

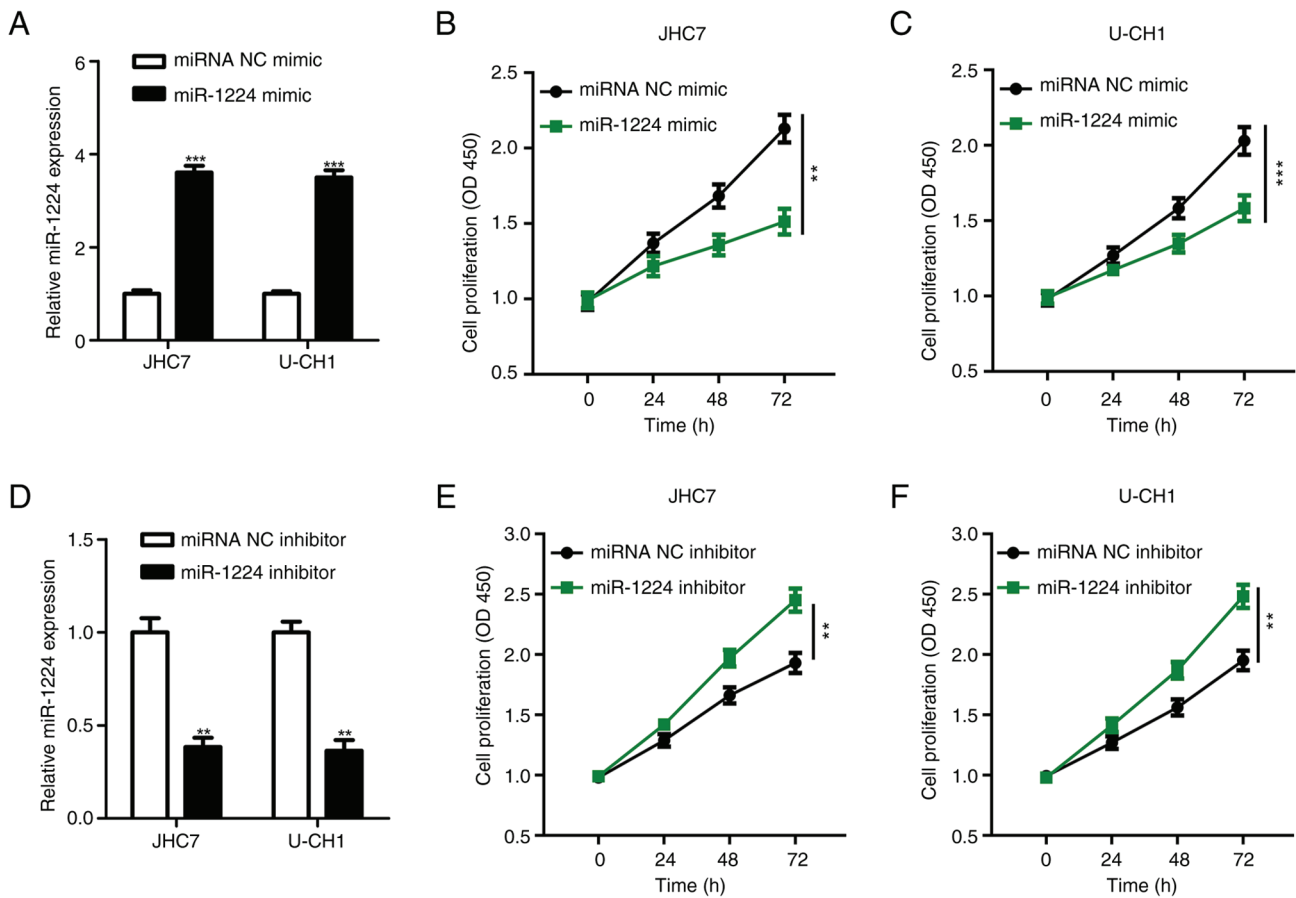


Figure 2. Verification efficiency of (A) miR-1224 mimic and (D) miR-1224 inhibitor in JHC7 and U-CH1 cell lines by reverse transcription-quantitative PCR. After the overexpression of miR-1224 in (B) JHC7 and (C) U-CH1 cells, the cell proliferation was detected by CCK-8. After knockdown of miR-1224 in (E) JHC7 and (F) U-CH1 cells, the cell proliferation was detected by CCK-8. ** $P < 0.01$ and *** $P < 0.001$. miR, microRNA.

significantly decreased the luciferase signal compared with the control. However, no significant decrease was seen with the MUT 3'-UTR (Fig. 3H). Thus, CBX3 is a direct target of miR-1224.

Effect of CBX3 on the proliferation ability of chordoma cells. CBX3 is highly expressed in numerous tumors and can promote tumor cell proliferation (17-20). Therefore, the expression of CBX3 was detected in chordoma cell lines and normal nucleus pulposus NP1 and NP2 cell lines. RT-qPCR demonstrated that the CBX3 mRNA was significantly increased in the JHC7 and U-CH1 cell lines compared with that in the nucleus pulposus cells (Fig. 4A). Western blotting showed that CBX3 protein was significantly increased in the JHC7 and U-CH1 cell lines compared with that in the nucleus pulposus cells (Fig. 4B).

Furthermore, the levels of CBX3 mRNA expression in JHC7 and U-CH1 cells were assessed following the transfection of CBX3 overexpression vector or CBX3 siRNA. The mRNA levels of CBX3 was significantly reduced in the chordoma JHC7 and U-CH1 cell lines transfected with the CBX3 siRNA compared with the control (Fig. 4C); this significantly reduced the proliferation ability of JHC7 (Fig. 4E) and U-CH1 (Fig. 4F) compared with the controls. Likewise, the mRNA level of CBX3 was significantly increased in the chordoma JHC7 and U-CH1 cell lines transfected with the CBX3 overexpression vector compared with the controls (Fig. 4D); this

significantly increased the proliferation of JHC7 (Fig. 4G) and U-CH1 (Fig. 4H) chordoma cell lines compared with the controls.

miR-1224 targets CBX3 and inhibit the proliferation of chordoma cells. To determine the functional relationship between miR-1224 and its potential target CBX3, and whether it is a functional target gene of miR-1224, a functional recovery experiment was further designed. The miR-1224 mimic and CBX3 overexpression plasmid were transfected into chordoma JHC7 and U-CH1 cells and divided into the following four groups: miRNA NC mimic + pMSCV-puro NC, miR-1224 mimic + pMSCV-puro NC, miRNA NC mimic + CBX3 overexpression (CBX3-OE) and miR-1224 mimic + CBX3-OE. RT-qPCR showed that the expression levels of miR-1224 was significantly increased in miR-1224 mimic + control group and miR-1224 mimic + CBX3 overexpression group compared with that in the other groups in the JHC7 and U-CH1 cells (Fig. 5A). RT-qPCR also showed that the expression of CBX3 mRNA was significantly increased in miRNA NC mimic + CBX3 overexpression group and the miR-1224 mimic + CBX3 overexpression group compared with that in the other groups in the JHC7 and U-CH1 cells, and that the expression of CBX3 mRNA was significantly decreased in the miR-1224 mimic + control group compared with that in the other groups (Fig. 5B). Western blotting demonstrated that the expression of CBX3

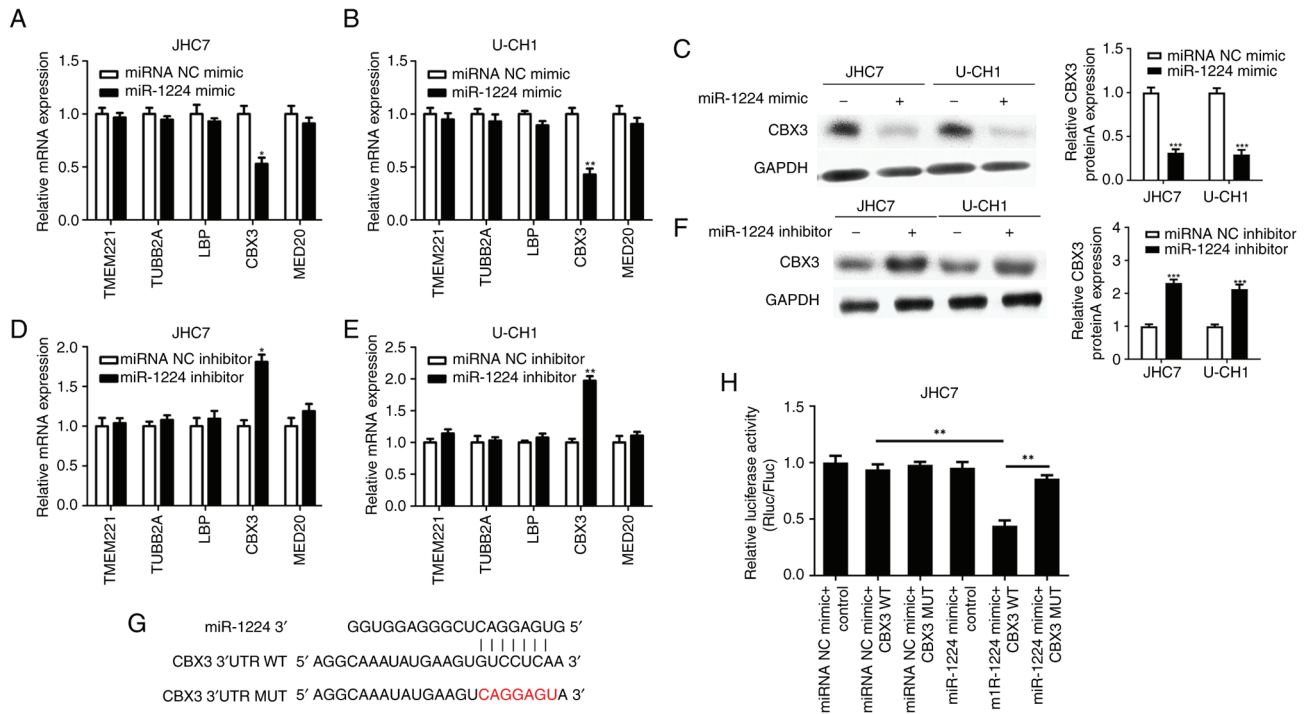


Figure 3. mRNA expression level of candidate target genes analyzed by RT-qPCR after the upregulation of miR-1224 expression in (A) JHC7 and (B) U-CH1 cell lines. The protein expression of CBX3 was analyzed by western blotting after the (C) upregulation and (F) knockdown of miR-1224 in JHC7 and U-CH1 cell lines compared with the miRNA NC mimic or miRNA NC inhibitor. The mRNA expression level of each candidate target genes was analyzed by RT-qPCR after the knockdown of miR-1224 in JHC7 (D) and U-CH1 (E) cell lines. (G) Sequences used in the dual luciferase reporter assay, showing the miR-1224, CBX3 3'UTR WT and CBX3 3'UTR MUT sequences. (H) A luciferase reporter assay was used to verify the direct binding between miR-1224 and CBX3. * $P < 0.05$, ** $P < 0.01$ and *** $P < 0.001$. WT, wild-type; MUT, mutant; UTR, untranslated region; RT-qPCR, reverse transcription-quantitative PCR; miR, microRNA; Rluc, *Renilla* luciferase; Fluc, *Firefly* luciferase.

protein was significantly increased in the miRNA NC mimic + CBX3 overexpression group and the miR-1224 mimic + CBX3 overexpression group compared with that in the other groups in the JHC7 and U-CH1 cells, and the expression of CBX3 protein was significantly decreased in the miR-1224 mimic + control group compared with that in the other groups (Fig. 5C).

Furthermore, the CCK-8 proliferation assay demonstrated that the cell proliferation was significantly increased in the miR-1224 mimic + CBX3 overexpression group compared with that in the miRNA NC mimic + control group, and that the cell proliferation was significantly decreased in the miR-1224 mimic + control group compared with that in the miRNA NC mimic + control group in the JHC7 (Fig. 5D) and U-CH1 (Fig. 5E) cells. Although the mRNA and protein levels of CBX3 detected in the miR-1224 mimic + CBX3 cell group were lower compared with the miRNA NC mimic + CBX3 group, there was no statistically significant difference (Fig. 5B). Likewise, there was no significant difference in the proliferation ability between the two groups (Fig. 5D and E). It was demonstrated that CBX3 overexpression can reverse the decrease in the proliferation caused by miR-1224.

Discussion

Chordoma originates from the residual chordoma tissues of the embryo and is a moderate- to low-grade malignant bone tumor, accounting for 1-4% of primary malignant bone tumors (1). Chordoma has no obvious clinical symptoms in the early stages of onset, grows slowly and has a long course

of disease. The tumor is often large and often accompanied by bone destruction or invasion of adjacent soft-tissue structures when detected (21). However, chordoma has a complex local anatomy near important neural vasculature, so surgical removal is difficult. Therefore, chordoma has a poor prognosis, with a postoperative recurrence rate as high as 30-85% (22). It is estimated that ~20% of chordomas will relapse within 1 year after surgery and 40-60% of patients will have distant metastasis. The 5-year survival rate of patients is 47-80% (3,23). The molecular mechanisms of proliferation and invasion in chordoma remain unclear. The biological role of miRNAs in tumors has gradually become a popular research topic. miRNAs can inhibit mRNA translation, directly degrade mRNA, inhibit target gene expression at the post-transcriptional level and serve a role in the proliferation, invasion and metastasis of malignant tumors. miRNAs can simultaneously regulate multiple target genes and serve key roles in the signal regulation network of tumorigenesis and tumor development, making them promising novel targets for molecular targeted therapy of malignant tumors (9,24-27). Previous studies have reported that numerous miRNAs, including miR-31, miR-185-5p, miR-125b-5p, miR-1260a, miR-1290 and miR-637 (28-30), are abnormally expressed in chordoma. In the present study, miR-1224 had the largest differential expression in chordoma tissues compared with notochord tissues, and its expression was significantly downregulated in chordoma tissues (GEO database) and cell lines. Knockdown of miR-1224 increased the proliferation of chordoma cells, while the overexpression of miR-1224 reduced the proliferation of chordoma cells. The

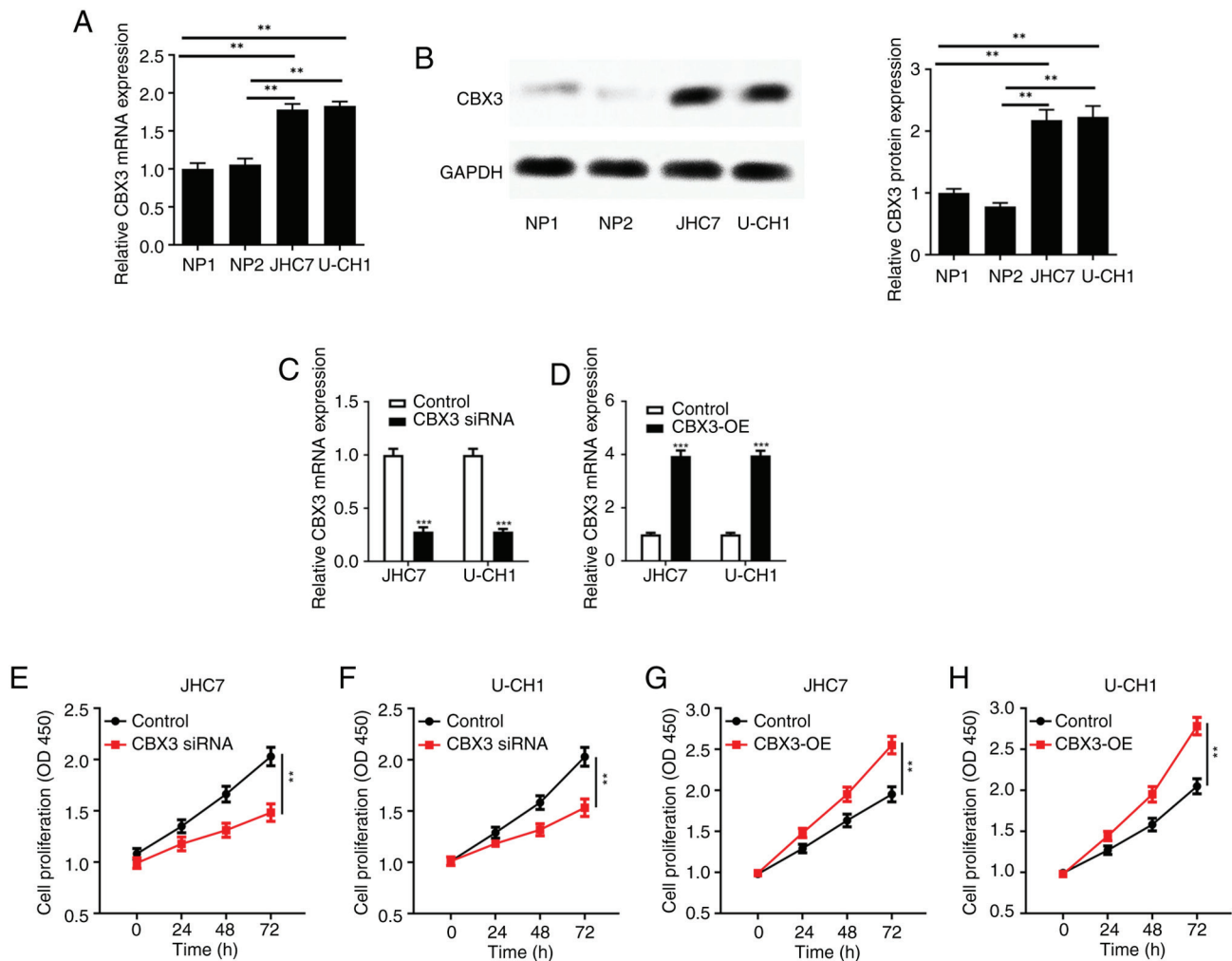


Figure 4. Detection of differences in CBX3 (A) mRNA and (B) protein expression in chordoma JHC7 and U-CH1 cell lines, and normal NP1 and NP2 cell lines. Verification efficiency of (C) knockdown and (D) overexpressed CBX3 in JHC7 and U-CH1 cell lines by reverse transcription-quantitative PCR. After knockdown of CBX3 in (E) JHC7 and (F) U-CH1, the cell proliferation was detected by CCK-8. After overexpression of CBX3 in (G) JHC7 and (H) U-CH1, the cell proliferation was detected by CCK-8. ** $P < 0.01$ and *** $P < 0.001$. siRNA, small interfering RNA.

forementioned findings suggest that miR-1224 serves a role as a tumor suppressor gene in chordoma. Several previous studies have reported that miR-1224 also serves a role as a tumor suppressor gene in a variety of tumors. For example, Mosakhani *et al* (31) studied the differential miRNA expression in 99 patients with metastatic colorectal cancer and reported that the downregulation of miR-1224 was correlated with poor patient survival. Scarpati *et al* (32) performed a microarray analysis of 38 patients with rectal cancer who underwent surgery and reported 14 abnormally expressed miRNAs, of which miR-1224 was significantly upregulated. Qian *et al* (33) studied 198 glioma samples and the Chinese Genome Map, and reported that miR-1224 has a lower expression level compared with other miRNAs in low-grade gliomas, and that miR-1224 can reduce the proliferative capacity of malignant gliomas by targeting CREB1 (33). Furthermore, in gastric cancer, miR-1224 inhibits the metastasis of gastric cancer cells by inhibiting the FAK-mediated STAT3 and NF- κ B signaling pathways (34).

In the present study, bioinformatics and dual reporter luciferase assays confirmed that miR-1224 directly targeted CBX3 mRNA, and miR-1224 inhibited CBX3 to inhibit the

proliferation of chordoma cells. CBX3 is a member of the heterochromatin protein 1 family and its chromatin binding domain can recognize the methylated histone H3K9 with the assistance of the histone methyltransferase uv339H1, thereby regulating gene expression (35-37). The combination of CBX3 and methylated H3K9 can recruit various cofactors to participate in a variety of biological processes of cells, including telomere metabolism, DNA damage repair, RNA splicing, transcription extension, transcription inhibition and activation (38). Previous studies reported that CBX3 is closely related to numerous human cancer types, including lung cancer, colon cancer, osteosarcoma and prostate cancer (17-20). For example, Alam *et al* (17) reported that CBX3 is the most commonly overexpressed and amplified histone reader protein in human lung adenocarcinoma, and that high CBX3 mRNA levels are associated with a poor prognosis in patients with lung adenocarcinoma. The study also reported that CBX3 binding to methylated histone H3K9 is necessary for the proliferation and migration of lung adenocarcinoma cells. Liu *et al* (18) reported that CBX3 expression is significantly upregulated in human colorectal cancer and can promote colorectal cancer cell proliferation *in vitro* and *in vivo*. Likewise, Ma *et al* (19) reported that CBX3 is highly expressed

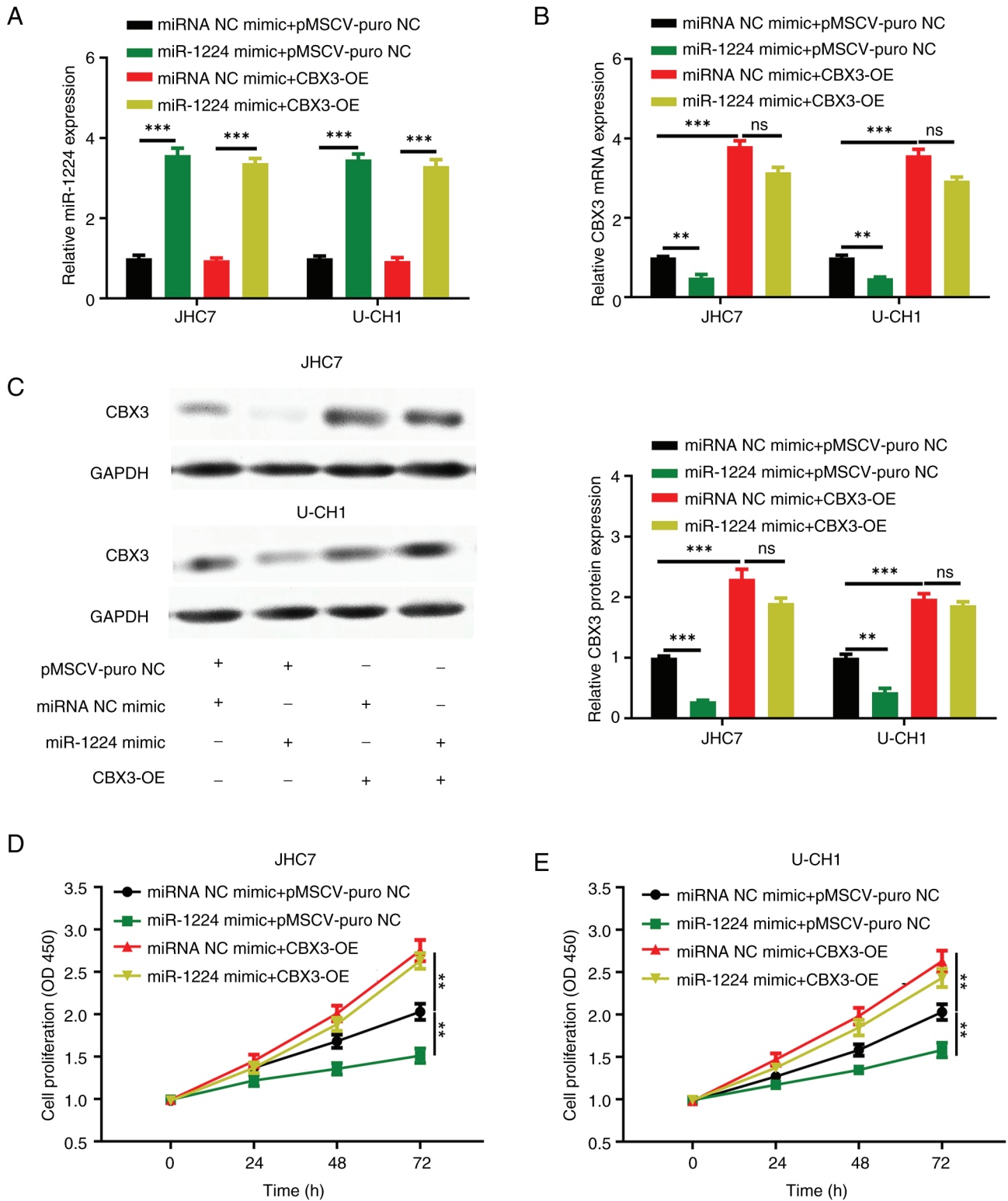


Figure 5. Reverse transcription-quantitative PCR of (A) miR-1224 and (B) CBX3 mRNA expression, (C) western blotting of CBX3 protein expression, and cell proliferation detected by Cell Counting Kit-8 in (D) JHC7 and (E) U-CH1 cell lines transfected with the following groups: miRNA NC mimic + pMSCV-puro NC, miR-1224 mimic + pMSCV-puro NC, miRNA NC mimic + CBX3-OE or miR-1224 mimic + CBX3-OE. **P<0.01 and ***P<0.001. NC, negative control; miR, microRNA.

in human osteosarcoma tissues. Furthermore, high CBX3 mRNA expression is a predictor of a poor prognosis in patients with osteosarcoma (19). Moreover, downregulating the expression of CBX can significantly reduce the proliferation capacity of osteosarcoma cells and lead to increased apoptosis and cell

cycle arrest in the G₀ and G₁ phases in osteosarcoma cells (19). Chang *et al* (20) reported that CBX3 is upregulated in prostate cancer, and the elevated CBX3 level in prostate cancer indicates a poor patient prognosis, while downregulating the expression of CBX3 in prostate cancer cells can significantly inhibit their

proliferation and induce apoptosis. The aforementioned results, and the results of the present study, indicate that CBX3 is an oncogene in tumors.

Due to the difficulty in constructing a chordoma animal model, no animal experiments were performed. This is a limitation of the present study. To the best of our knowledge, the present study was the first to have verified the role of miR-1224 in chordoma and confirmed the mechanism of miR-1224-suppressed chordoma cell proliferation by inhibiting the target gene CBX3. The results of the present study provide a novel therapeutic target and theoretical basis for the treatment of chordoma.

Acknowledgements

Not applicable.

Funding

No funding was received.

Availability of data and material

The data generated in the present study may be requested from the corresponding author.

Authors' contributions

WX and KY conceived and designed the study, and drafted the manuscript. JH, CS and FS performed the experiments. WX and KY confirm the authenticity of all the raw data. JH and CS performed the statistical analysis. All authors read and approved the final version of the manuscript.

Ethics approval and consent to participate

Not applicable.

Patient consent for publication

Not applicable.

Competing interests

The authors declare that they have no competing interests.

References

- Walcott BP, Nahed BV, Mohyeldin A, Coumans JV, Kahle KT and Ferreira MJ: Chordoma: Current concepts, management, and future directions. *Lancet Oncol* 13: e69-e76, 2012.
- Pan Y, Lu L, Chen J, Zhong Y and Dai Z: Analysis of prognostic factors for survival in patients with primary spinal chordoma using the SEER Registry from 1973 to 2014. *J Orthop Surg Res* 13: 76, 2018.
- Kayani B, Hanna SA, Sewell MD, Saifuddin A, Molloy S and Briggs TW: A review of the surgical management of sacral chordoma. *Eur J Surg Oncol* 40: 1412-1420, 2014.
- Le Cesne A, Chevreau C, Perrin C, Italiano A, Hervieu A, Blay JY, Piperno-Neumann S, Saada-Bouزيد E, Bertucci F, Firmin N, *et al*: Regorafenib in patients with relapsed advanced or metastatic chordoma: Results of a non-comparative, randomised, double-blind, placebo-controlled, multicentre phase II study. *ESMO Open* 8: 101569, 2023.
- Bartel DP: MicroRNAs: Genomics, biogenesis, mechanism, and function. *Cell* 116: 281-297, 2004.
- Liu H, Lei C, He Q, Pan Z, Xiao D and Tao Y: Nuclear functions of mammalian MicroRNAs in gene regulation, immunity and cancer. *Mol Cancer* 17: 64, 2018.
- Rupaimoole R and Slack FJ: MicroRNA therapeutics: Towards a new era for the management of cancer and other diseases. *Nat Rev Drug Discov* 16: 203-222, 2017.
- Breulmann FL, Hatt LP, Schmitz B, Wehrle E, Richards RG, Bella ED and Stoddart MJ: Prognostic and therapeutic potential of microRNAs for fracture healing processes and non-union fractures: A systematic review. *Clin Transl Med* 13: e1161, 2023.
- Shao Y, Song X, Jiang W, Chen Y, Ning Z, Gu W and Jiang J: MicroRNA-621 acts as a tumor radiosensitizer by directly targeting SETDB1 in hepatocellular carcinoma. *Mol Ther* 27: 355-364, 2019.
- Shao Y, Zhang D, Li X, Yang J, Chen L, Ning Z, Xu Y, Deng G, Tao M, Zhu Y and Jiang J: MicroRNA-203 increases cell radiosensitivity via directly targeting Bmi-1 in hepatocellular carcinoma. *Mol Pharm* 15: 3205-3215, 2018.
- Shi L, Zhu W, Huang Y, Zhuo L, Wang S, Chen S, Zhang B and Ke B: Cancer-associated fibroblast-derived exosomal microRNA-20a suppresses the PTEN/PI3K-AKT pathway to promote the progression and chemoresistance of non-small cell lung cancer. *Clin Transl Med* 12: e989, 2022.
- Li H, Zhang N, Jiao X, Wang C, Sun W, He Y, Ren G, Huang S, Li M, Chang Y, *et al*: Downregulation of microRNA-6125 promotes colorectal cancer growth through YTHDF2-dependent recognition of N6-methyladenosine-modified GSK3 β . *Clin Transl Med* 11: e602, 2021.
- Liu Z, Wu K, Gu S, Wang W, Xie S, Lu T, Li L, Dong C, Wang X and Zhou Y: A methyltransferase-like 14/miR-99a-5p/tribble 2 positive feedback circuit promotes cancer stem cell persistence and radioresistance via histone deacetylase 2-mediated epigenetic modulation in esophageal squamous cell carcinoma. *Clin Transl Med* 11: e545, 2021.
- Long C, Jiang L, Wei F, Ma C, Zhou H, Yang S, Liu X and Liu Z: Integrated miRNA-mRNA analysis revealing the potential roles of miRNAs in chordomas. *PLoS One* 8: e66676, 2013.
- Livak KJ and Schmittgen TD: Analysis of relative gene expression data using real-time quantitative PCR and the 2(-Delta Delta C(T)) method. *Methods* 25: 402-408, 2001.
- Hu L, Xie X, Xue H, Wang T, Panayi AC, Lin Z, Xiong Y, Cao F, Yan C, Chen L, *et al*: MiR-1224-5p modulates osteogenesis by coordinating osteoblast/osteoclast differentiation via the Rap1 signaling target ADCY2. *Exp Mol Med* 54: 961-972, 2022.
- Alam H, Li N, Dhar SS, Wu SJ, Lv J, Chen K, Flores ER, Baseler L and Lee MG: HPI γ promotes lung adenocarcinoma by downregulating the transcription-repressive regulators NCOR2 and ZBTB7A. *Cancer Res* 78: 3834-3848, 2018.
- Liu M, Huang F, Zhang D, Ju J, Wu XB, Wang Y, Wang Y, Wu Y, Nie M, Li Z, *et al*: Heterochromatin protein HPI γ promotes colorectal cancer progression and is regulated by miR-30a. *Cancer Res* 75: 4593-4604, 2015.
- Ma C, Nie XG, Wang YL, Liu XH, Liang X, Zhou QL and Wu DP: CBX3 predicts an unfavorable prognosis and promotes tumorigenesis in osteosarcoma. *Mol Med Rep* 19: 4205-4212, 2019.
- Chang C, Liu J, He W, Qu M, Huang X, Deng Y, Shen L, Zhao X, Guo H, Jiang J, *et al*: A regulatory circuit HPI γ /miR-451a/c-Myc promotes prostate cancer progression. *Oncogene* 37: 415-426, 2018.
- Pamir MN and Ozduman K: Tumor-biology and current treatment of skull-base chordomas. *Adv Tech Stand Neurosurg* 33: 35-129, 2008.
- Huo X, Ma S, Wang C, Song L, Yao B, Zhu S, Li P, Wang L, Wu Z and Wang K: Unravelling the role of immune cells and FN1 in the recurrence and therapeutic process of skull base chordoma. *Clin Transl Med* 13: e1429, 2023.
- Hanna SA, Aston WJ, Briggs TW, Cannon SR and Saifuddin A: Sacral chordoma: Can local recurrence after sacrectomy be predicted? *Clin Orthop Relat Res* 466: 2217-2223, 2008.
- Volinia S, Calin GA, Liu CG, Ambs S, Cimmino A, Petrocca F, Visone R, Iorio M, Roldo C, Ferracin M, *et al*: A microRNA expression signature of human solid tumors defines cancer gene targets. *Proc Natl Acad Sci USA* 103: 2257-2261, 2006.
- Iorio MV and Croce CM: microRNA involvement in human cancer. *Carcinogenesis* 33: 1126-1133, 2012.

26. Ma YS, Yu F, Zhong XM, Lu GX, Cong XL, Xue SB, Xie WT, Hou LK, Pang LJ, Wu W, *et al*: miR-30 family reduction maintains self-renewal and promotes tumorigenesis in NSCLC-initiating cells by targeting oncogene TM4SF1. *Mol Ther* 26: 2751-2765, 2018.
27. Slater SC, Jover E, Martello A, Mitić T, Rodriguez-Arabaolaza I, Vono R, Alvino VV, Satchell SC, Spinetti G, Caporali A and Madeddu P: MicroRNA-532-5p regulates pericyte function by targeting the transcription regulator BACH1 and angiopoietin-1. *Mol Ther* 26: 2823-2837, 2018.
28. Bayrak OF, Gulluoglu S, Aydemir E, Ture U, Acar H, Atalay B, Demir Z, Sevli S, Creighton CJ, Ittmann M, *et al*: MicroRNA expression profiling reveals the potential function of microRNA-31 in chordomas. *J Neurooncol* 115: 143-151, 2013.
29. Chen K, Chen H, Zhang K, Sun S, Mo J, Lu J, Qian Z and Yang H: MicroRNA profiling and bioinformatics analyses reveal the potential roles of microRNAs in chordoma. *Oncol Lett* 14: 5533-5539, 2017.
30. Huo X, Wang K, Yao B, Song L, Li Z, He W, Li Y, Ma J, Wang L and Wu Z: Function and regulation of miR-186-5p, miR-125b-5p and miR-1260a in chordoma. *BMC Cancer* 23: 1152, 2023.
31. Mosakhani N, Lahti L, Borze I, Karjalainen-Lindsberg ML, Sundström J, Ristamäki R, Osterlund P, Knuutila S and Sarhadi VK: MicroRNA profiling predicts survival in anti-EGFR treated chemorefractory metastatic colorectal cancer patients with wild-type KRAS and BRAF. *Cancer Genet* 205: 545-551, 2012.
32. Scarpati GD, Falcetta F, Carlomagno C, Ubezio P, Marchini S, De Stefano A, Singh VK, D'Incalci M, De Placido S and Pepe S: A specific miRNA signature correlates with complete pathological response to neoadjuvant chemoradiotherapy in locally advanced rectal cancer. *Int J Radiat Oncol Biol Phys* 83: 1113-1119, 2012.
33. Qian J, Li R, Wang YY, Shi Y, Luan WK, Tao T, Zhang JX, Xu YC and You YP: MiR-1224-5p acts as a tumor suppressor by targeting CREB1 in malignant gliomas. *Mol Cell Biochem* 403: 33-41, 2015.
34. Wang J, Wen T, Li Z, Che X, Gong L, Yang X, Zhang J, Tang H, He L, Qu X and Liu Y: MicroRNA-1224 inhibits tumor metastasis in intestinal-type gastric cancer by directly targeting FAK. *Front Oncol* 9: 222, 2019.
35. Canzio D, Larson A and Narlikar GJ: Mechanisms of functional promiscuity by HP1 proteins. *Trends Cell Biol* 24: 377-386, 2014.
36. Mishima Y, Jayasinghe CD, Lu K, Otani J, Shirakawa M, Kawakami T, Kimura H, Hojo H, Carlton P, Tajima S and Suetake I: Nucleosome compaction facilitates HP1 γ binding to methylated H3K9. *Nucleic Acids Res* 43: 10200-10212, 2015.
37. Bannister AJ, Zegerman P, Partridge JF, Miska EA, Thomas JO, Allshire RC and Kouzarides T: Selective recognition of methylated lysine 9 on histone H3 by the HP1 chromo domain. *Nature* 410: 120-124, 2001.
38. Cheutin T, McNairn AJ, Jenuwein T, Gilbert DM, Singh PB and Misteli T: Maintenance of stable heterochromatin domains by dynamic HP1 binding. *Science* 299: 721-725, 2003.



Copyright © 2024 Xia et al. This work is licensed under a Creative Commons Attribution-NonCommercial-NoDerivatives 4.0 International (CC BY-NC-ND 4.0) License.